High temperature stress relaxation of a Ni-based single-crystal superalloy

Mikael Segersäll[1,*], Johan J. Moverare[1,2], Daniel Leidermark[1], Kjell Simonsson[1]

[1] Department of Management and Engineering, Linköping University, Linköping SE-58183, Sweden
[2] Siemens Industrial Turbomachinery AB, Finspång SE-61283, Sweden
* Corresponding author: mikael.segersall@liu.se

Abstract Nickel-based superalloys are often selected due to their remarkable mechanical and chemical properties at high temperatures. This makes the material suitable for high temperature applications such as gas turbines and aero engines. By use of single-crystal instead of poly-crystal material, both creep and fatigue properties are enhanced. Superalloys in single-crystal form exhibit an anisotropic behaviour and a tension/compression asymmetry. This makes it interesting to study different crystal orientations in both tension and compression. In this study, high temperature stress relaxation of a Ni-based single-crystal superalloy is investigated. Specimens with three different crystal orientations, ⟨001⟩, ⟨011⟩ and ⟨111⟩, were tested in both tension and compression. Results show an anisotropic stress relaxation behaviour, as well as a tension/compression asymmetry for all directions. During stress relaxation at 750°C, the creep properties decreases in the sequence ⟨001⟩, ⟨011⟩ and ⟨111⟩ in tension, while in compression ⟨001⟩ = ⟨011⟩, ⟨111⟩. However, at 950°C the creep properties are slightly better in the ⟨011⟩ direction compared to the ⟨001⟩ direction.

Keywords single-crystal superalloy, thermomechanical fatigue, stress relaxation

1. Introduction

Ni-based superalloys show remarkable mechanical and chemical properties at high temperatures, which make them a suitable as blade material in gas turbines and aero engines [1, 2]. The superalloys consist of the typical γ/γ′-microstructure, where the γ′-phase works as strengthener in a matrix of γ. The strengthening γ′-phase has an $L1_2$-ordered structure and is rich of Al, Ta and Ti. By using a single-crystal material instead of poly-crystal material both creep and fatigue properties are enhanced [3]. Gas turbine blades in single-crystal form are most common casted with the ⟨001⟩ crystallographic direction upwards, since this direction has the lowest stiffness of all crystal directions. Low stiffness implies good fatigue properties, which is of great importance for gas turbine blade components. Single-crystal superalloys exhibit an anisotropic behaviour and they also show a tension/compression asymmetry [4-7] .

Stress relaxation testing of superalloys is often associated with shorter hold times at high temperatures during thermomechanical fatigue (TMF) testing, for example hold times of 5 min during each cycle [8, 9]. However, Zhang et al. [10] applied a hold time of 1h at 900°C in compression at each cycle during TMF testing. In that study, three different stages of stress relaxation during the TMF tests were found, and each stage was connected to a specific microstructural behaviour. Other research showed that when applying hold times of 30-60 minutes during tensile loadings at temperatures from 700 to 1000°C, the stress relaxed to an asymptotic stress value after the hold time [11]. At high temperatures and loads a directional coarsening of the γ/γ′-microstructure is obtained. This phenomenon is called rafting and it is a diffusion controlled directional coarsening of the γ′-particles [12]. The orientation of the rafting is dependent on whether the alloy has a positive or negative lattice misfit [13]. Rafting doesn't always have to be negative for the material. For instance, research has shown how pre-rafting can improve creep properties [14]. Also isothermal high-temperature fatigue lives have proven to be enhanced by a pre-rafted microstructure, instead of having the more common microstructure with γ′-cuboids in a γ-matrix [15, 16].

The aim of this study is to investigate the long-term stress relaxation behaviour of a Ni-based single-crystal superalloy. Due to anisotropy and the well-known tension/compression asymmetry, three different crystal orientations are tested in both tension and compression.

2. Experimental procedure

The Ni-based single-crystal superalloy MD2 with chemical composition Ni-5.1Co-6.0Ta-8.0Cr-8.1W-5.0Al-1.3Ti-2.1Mo-0.1Hf-0.1Si in wt.%, was used in this study. Prior testing, the material was solution heat treated at 1275°C for 8 h followed by a two-stage aging process with 3 h at 1100°C and 24 h at 850°C. Test specimens were machined from cast bars and the deviation from the ideal orientation was less than 10° for all specimens.

The tests were performed in an Instron servo-hydraulic TMF machine, and were conducted as strain controlled TMF cycles with a temperature range from 100°C to either 750°C or 950°C. During each cycle, a hold time of 100 h was applied at maximum temperature (T_{max}) and maximum strain. After the 100 h hold time, the temperature was lowered to 100°C and zero strain before the second cycle was initiated. Each specimen was subjected to two TMF cycles, and no specimens were cycled to fracture. Consequently, a hold time of total 200 h at T_{max} was applied for each specimen. Fig. 1 displays a plot of the TMF cycle. For a T_{max} of 750°C, the ⟨001⟩, ⟨011⟩ and ⟨111⟩ directions were tested. However, for a T_{max} of 950°C, only the ⟨001⟩ and ⟨011⟩ directions were tested. The total mechanical strain range ($\Delta\varepsilon_{mech}$) was chosen in order to obtain approximately the same inelastic strain for all specimens. Since the different crystal orientations have different Young's modulus, different $\Delta\varepsilon_{mech}$ were used for the different crystal directions. The ⟨001⟩ oriented specimens were subjected to a $\Delta\varepsilon_{mech}$ of 1%, the ⟨011⟩ specimens to 0.7%, and the ⟨111⟩ specimens were subjected to 0.6%. For each direction and T_{max}, one specimen was subjected to an in-phase TMF cycle (IP-TMF), and the other specimen was subjected to an out-of-phase TMF cycle (OP-TMF). An IP-TMF cycle implies tensile stress relaxation at T_{max} while OP-TMF implies compressive stress relaxation at T_{max}.

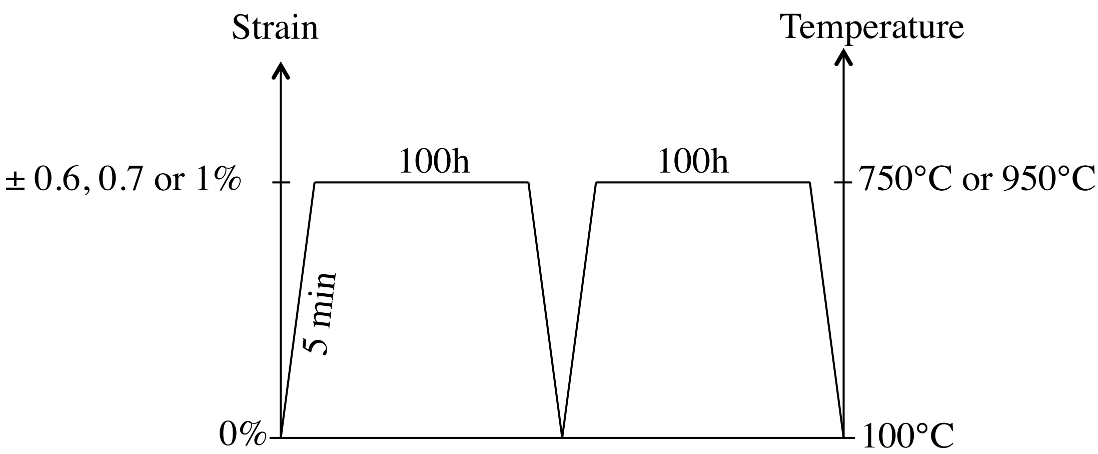

Figure 1. The TMF cycle used in the stress relaxation tests.

After the tests, all specimens were examined by stereomicroscopy before they were cut parallel to the loading direction for further microstructural investigation by scanning electron microscopy (SEM). The SEM samples were prepared by grinding and mechanical polishing, but no samples were etched. The microstructure investigation was performed in a Hitachi SU70 SEM, using voltages from 10 to 20 kV.

3. Results

3.1. Stress relaxation testing

Results from the tests with a T_{max} of 750°C show that the ⟨011⟩ oriented specimens demonstrates a serrated yielding behaviour during the loading phase. This was visible in both tension (IP) and compression (OP). However, the yielding for both the ⟨001⟩ and ⟨111⟩ directions during the loading phase was more stable, i.e. no serrated yielding was observed. In addition to the serrated yielding for the ⟨011⟩ direction, those specimens also demonstrated a clear noise during the loading phase. On the other hand, both the ⟨001⟩ and ⟨111⟩ directions were more quite. For the specimens subjected to stress relaxation at T_{max} of 950°C no serrated yielding and no noise was observed during the loading phase.

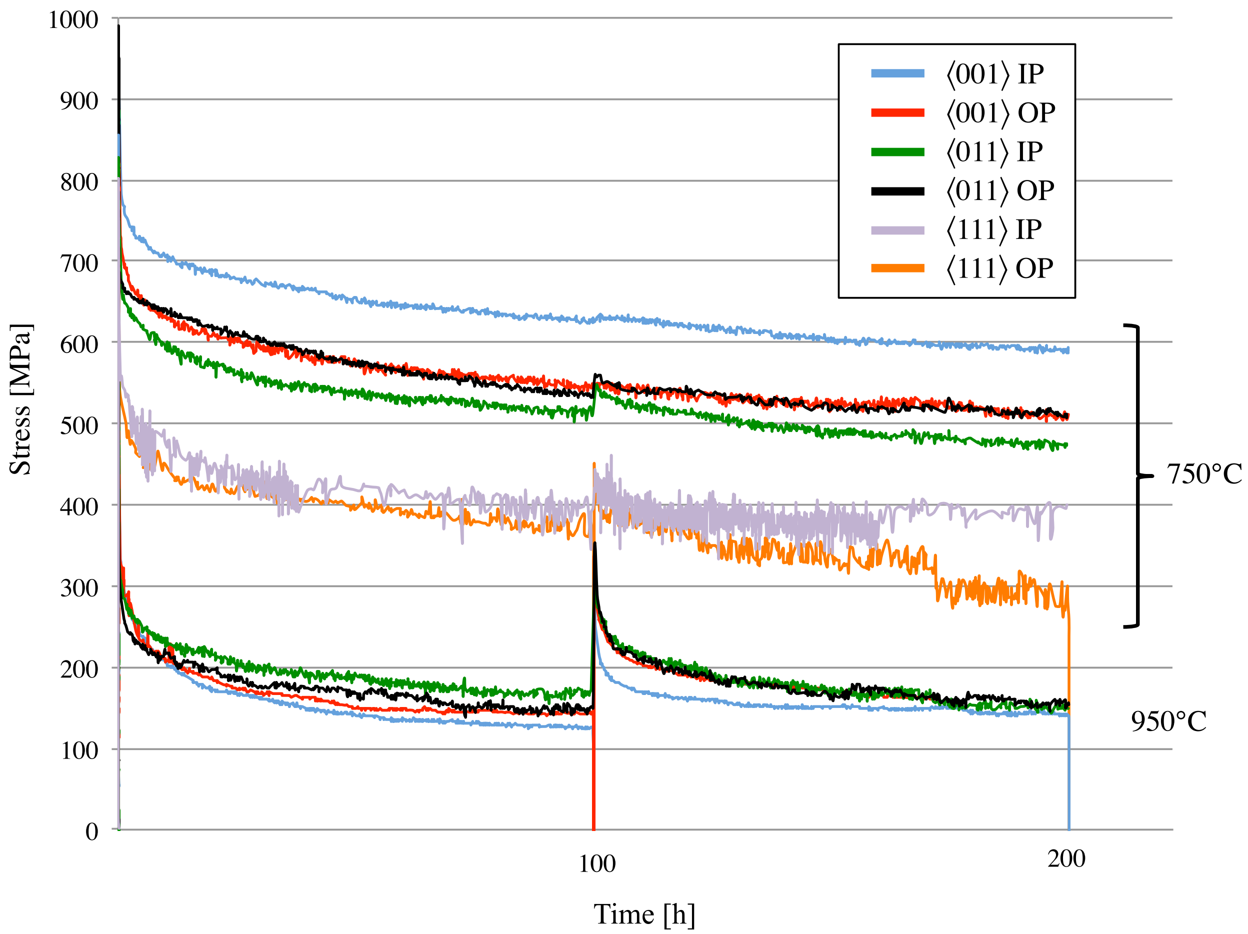

Figure. 2. Stress relaxation over 200 h for all crystal orientations tested.

Fig. 2 displays how the stress is relaxing during the 200 h hold time for all specimens. The figure shows that the stresses relax to lower stress states at 950°C compared to 750°C. The other significant differences in the stress relaxation behaviour are summarized below.

All crystal orientations show a tension/compression asymmetry. However, the asymmetry is most pronounced the ⟨001⟩ direction at 750°C. Here, tensile loading leads to a higher stress state compared to compressive loading, and the difference in stress is approximately 80 MPa after 200 h. The ⟨011⟩ oriented specimens show an opposite behaviour at this temperature; tensile loading leads to a lower stress state compared to compressive loading. Another difference at this temperature, is that the unloading after 100 h leads to an increase in stress state for the ⟨011⟩ direction when the material is loaded into the second 100 h TMF cycle. However, after some time the material relaxes and adapts into the pre-unloading behaviour. For the ⟨001⟩ direction the unloading after 100 h does not have an influence on the stress state.

Concerning the ⟨111⟩ oriented specimens, they relax to a significant lower stress state compared to both ⟨001⟩ and ⟨011⟩ directions. After the first 100 h TMF cycle, the stress is approximately 360 MPa for the ⟨111⟩ direction, while both ⟨001⟩ and ⟨011⟩ directions are well above 500 MPa. It should be noted that the stress relaxation in the ⟨111⟩ direction is very unstable compared to the other directions. The instability should be attributed to TMF machine instabilities, rather than any microstructural difference between the three directions. One reason can be that the high stiffness in the ⟨111⟩ direction makes it more difficult for the TMF machine to take care of instabilities.

At 950°C, only the ⟨001⟩ and ⟨011⟩ directions were tested. At this temperature, an opposite tension/compression asymmetry is observed compared to 750°C. The ⟨001⟩ direction is stronger in compression than tension, while the ⟨011⟩ direction is stronger in tension than compression. Here the unloading after 100 h also seems to influence the specimens to a greater extent compared to 750°C. A significant higher stress state is observed in the beginning of the second TMF cycle. This is the case for both ⟨001⟩ and ⟨011⟩ directions at 950°C, but only for the ⟨011⟩ direction at 750°C.

3.2. Microscopy

Crystallographic deformation bands across the specimens are found on the ⟨011⟩ oriented materials subjected to hold times at 750°C, both in tension (IP) and compression (OP). See Fig. 3a for the ⟨011⟩ oriented specimen subjected to 750°C in compression. Neither the ⟨001⟩ nor ⟨111⟩ oriented specimens show similar deformation bands at this temperature. However at 950°C, both ⟨001⟩ and ⟨001⟩ oriented specimens show crystallographic deformation bands (the ⟨111⟩ direction was not tested at this temperature). Another difference between the two temperatures is that the deformation bands become more distinct at 950°C compared to 750°C. All slip traces are consistent with slip along the {111}⟨110⟩ slip systems. In Fig. 3b, the more distinct deformation bands are visible. This figure shows the deformation bands on the ⟨011⟩ oriented specimen subjected to tensile stresses at 950°C. Here, slip traces on different {111} planes are found. In Fig. 3c, the deformation bands on the ⟨001⟩ oriented specimen subjected to tensile stresses are shown. In this case, in addition to the crystallographic deformation bands, also wavy deformation bands are found. This indicates that several slip systems are active during deformation in this direction at 950°C.

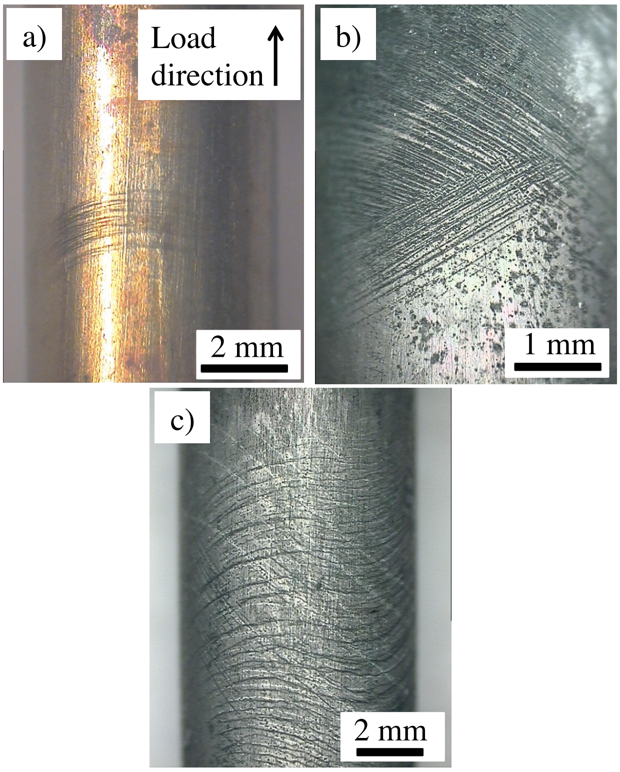

Figure. 3. Deformation bands on specimen surfaces, a) the ⟨011⟩ specimen subjected to 750°C in compression (OP), b) the ⟨011⟩ specimen subjected to 950°C in tension (IP), and c) the ⟨001⟩ specimen subjected to 950°C in tension (IP).

After cutting the specimens parallel to the loading direction all specimens were investigated by SEM. Fig. 4 provides a backscattered electron image where the deformation bands inside the specimen are clearly visible at low magnification. However, at higher magnification the crystallographic deformation bands are often difficult to detect. The SEM investigation shows that the deformation bands are neither twinning nor shearing of the γ/γ′-microstructure. Sometimes precipitation of topologically-close-packed (TCP) phases are visible within the deformation bands. Even though most deformation bands are difficult to detect at higher magnification, occasionally more distinct deformation bands are visible, see Fig. 5 for such a distinct deformation band. Most likely, both types of deformation bands are bundles of glide bands. Other than the crystallographic deformation bands, the specimens show very little deformation within the γ/γ′-microstructure. However, small amounts of twins are detected in the microstructure for the ⟨001⟩ specimen subjected to compression at 750°C, see Fig. 6. Here parallel twins propagates through the γ′-cuboids.

Rafting of the γ/γ′-microstructure is visible in specimens subjected to holdtimes at 950°C. The rafting direction is dependent on whether the superalloy has a negative or positive misfit between the γ′- and γ-microconstituents, and if the loading is tensile or compressive. The alloy used in this study (MD2) has a negative misfit which implies that tensile loaded specimens show a N-type of rafting, while material loaded in compression show a P-type of rafting. Fig. 7 displays N-type of rafting; the previously cuboidal γ′-particles are here coarsened and oriented Normal to the load direction. On the other hand, Fig. 5 shows P-type of rafting where the coarsened γ′-particles are oriented Parallel to the load direction.

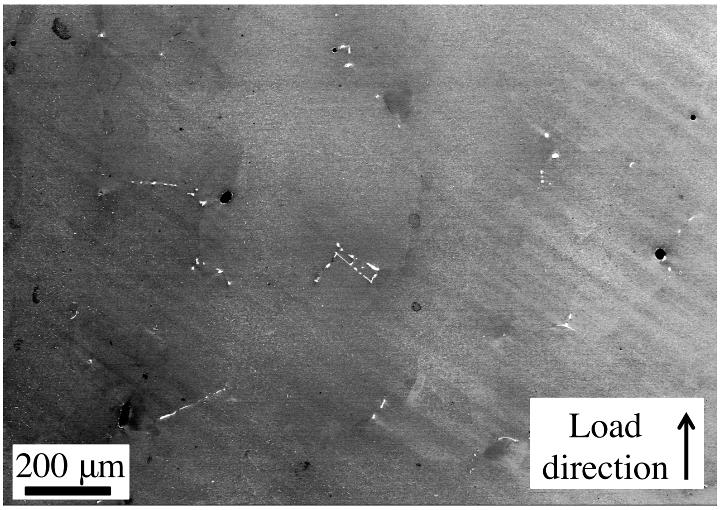

Figure. 4. Backscattered electron image of the ⟨011⟩ specimen subjected to stress relaxation tests at 950°C in tension (IP): crystallographic deformation bands at low magnification.

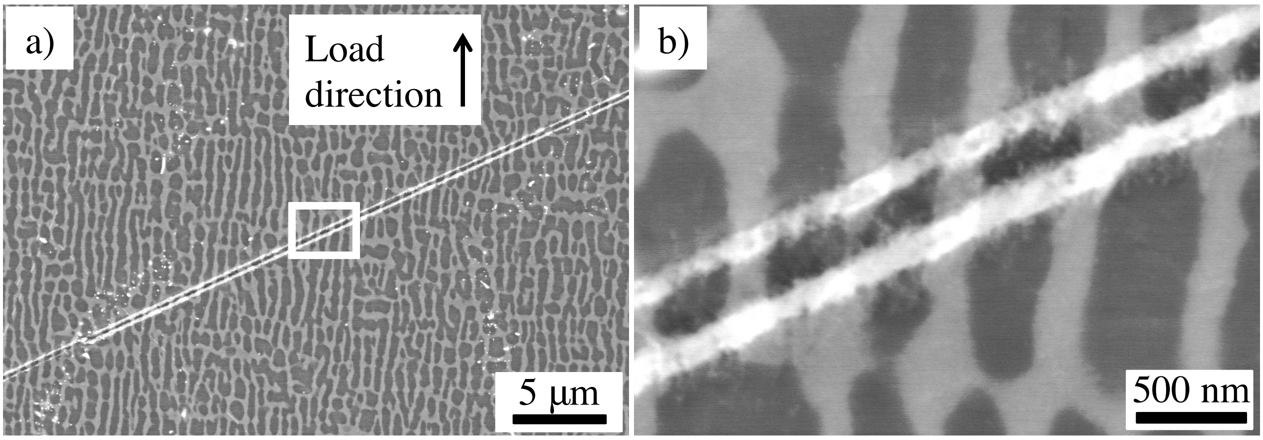

Figure. 5. Backscattered electron images of the ⟨011⟩ specimen subjected to stress relaxation tests at 950°C in compression (OP): a) distinct deformation band, b) magnification of a). P-type of rafting of the γ/γ'-microstructure.

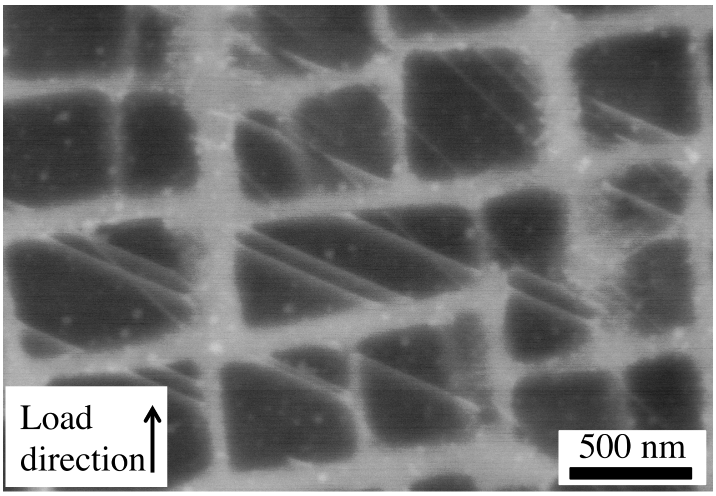

Figure. 6. Backscattered electron image of the ⟨001⟩ specimen subjected to stress relaxation tests at 750°C in compression (OP): twin formation in the γ/γ'-microstructure.

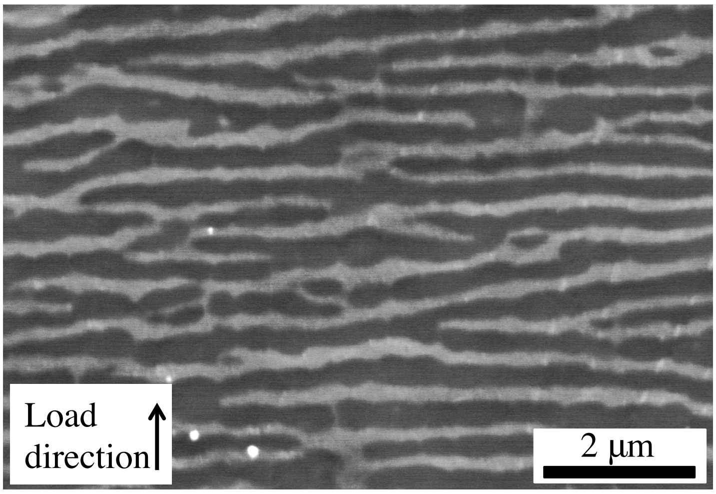

Figure. 7. Backscattered electron images of the ⟨001⟩ specimen subjected to stress relaxation test at 950°C in tension, N-type of rafting of the γ/γ′-microstructure.

4. Discussion

The MD2 alloy exhibits an anisotropic creep behaviour as well as a tension/compression asymmetry during stress relaxation, see Fig. 2. It can also be seen that the ⟨111⟩ direction has the worst creep properties at 750°C. This direction relaxes to a significant lower stress state compared to both ⟨001⟩ and ⟨011⟩ direction during the stress relaxation tests. At 750°C, the ⟨001⟩ and ⟨111⟩ specimens are stronger in tension than compression. However, for the ⟨011⟩ specimens the opposite behaviour is observed; compressive loading leads to a higher stress state compared to tensile loading. At 950°C, an opposite tension/compression asymmetry is observed: the ⟨001⟩ direction is stronger in compression than tension, and the ⟨011⟩ direction is stronger in tension than compression. It seems that there is a change in tension/compression asymmetry when going from 750°C to 950°C. That the tension/compression asymmetry changes with temperature has been showed by Ezz et al. [6] who studied the tension/compression asymmetry for the critical resolved shear stress (CRSS) for a single-crystal superalloy. They showed that the CRSS is higher in tension than compression at 750°C for orientations close to [001] in the stereographic triangle. On the other hand, for materials close to [011] and [111] in the stereographic triangle, there was a smaller asymmetry in CRSS at this temperature. At higher temperatures the asymmetry decreased. Present study shows that there is a change in tension/compression asymmetry also in stress relaxation behaviour, however the reason to this is still to be determined.

The ⟨011⟩ oriented specimens showed a serrated yielding behaviour during loading into the first TMF cycle in the tests at 750°C. This behaviour is attributed to two things; the fact that only one slip system is active during deformation in this direction and the effect of dynamic strain ageing (DSA). Serrated yielding behaviour of the ⟨011⟩ direction has previously been reported in the literature [17-20]. One explanation for this has been that only one slip system is active during deformation of the ⟨011⟩ direction while multiple slip systems are active during plastic deformation in the ⟨001⟩ direction [17]. The reason to single slip for the ⟨011⟩ direction is attributed to the lower symmetry, i.e. less equivalent slip systems, for this direction compared to the ⟨001⟩ and ⟨111⟩ directions. When several slip systems are active at the same time, there is always one slip system where the dislocations can propagate and a more stable yielding is observed. On the other hand, if only one slip system is active, the dislocations are sometimes stopped if the stress is not large enough and a more serrated yielding is obtained. The fact that deformation bands are found only on the ⟨011⟩ specimens at 750°C can also be attributed to the fact that only one slip system is active in this direction and temperature. The deformation bands on the surfaces are topographic differences, which are more probable to obtain when only one slip system is active compared to the case when several systems are active. This since slip on several systems will lead to a more homogeneous surface. The serrated yielding behaviour of the ⟨011⟩ direction at 750°C can also be attributed to dynamic strain aging (DSA). Localized deformation bands are found on these specimens, and those deformation bands are likely glide bands with a high dislocation density. DSA is the interaction between solute atoms and moving dislocations, and is favoured in areas with a high dislocation density, i.e. within those localized deformation bands.

A clear noise was heard from the ⟨011⟩ oriented specimens when loading into the first TMF cycle for tests at 750°C. This behaviour of the ⟨011⟩ direction has been reported before when acoustic emission (AE) was used to measure noise during plastic deformation [21]. In that study, loading in the ⟨011⟩ direction led to higher AE signals and higher noise compared to ⟨001⟩. It is thus likely, that during loading of the ⟨011⟩ direction at this temperature, in which serrated yielding occurs, a high noise is created for each serration.

4. Conclusions

From this study it can be concluded that the Ni-based single-crystal superalloy MD2 shows an anisotropic creep behaviour as well as a tension/compression asymmetry during stress relaxation. At 750°C, the tensile creep properties is best for the ⟨001⟩ direction, followed by the ⟨011⟩ direction while the ⟨111⟩ direction has the worst creep properties. At the same temperature in compression, the ⟨001⟩ and ⟨011⟩ directions show similar creep properties, and also here the ⟨111⟩ direction shows the worst creep properties. During stress relaxation at 950°C, the creep properties are slightly better in the ⟨011⟩ direction compared to the ⟨001⟩ direction for both compressive and tensile loadings.

Acknowledgements

The work has been financially supported by Siemens Industrial Turbomachinery AB in Finspång, Sweden and the Swedish Energy Agency, via the Research Consortium of Materials Technology for Thermal Energy Processes, Grant No. KME-502.

References

[1] R.C. Reed, T. Tao, N. Warnken, Alloys-By-Design: Application to nickel-based single crystal superalloys. Acta Materialia, 57 (2009) 5898-5913.

[2] T.M. Pollock, S. Tin, Nickel-based superalloys for advanced turbine engines: Chemistry, microstructure, and properties. J. Propul, Power. 22 (2006) 361-374.

[3] R.C. Reed, The Superalloys - Fundamentals and Applications, Cambridge University Press, Cambridge, 2006.

[4] N. Tsuno, S. Shimabayashi, K. Kakehi, C.M.F. Rae, R.C. Reed, Tension/compression asymmetry in yield and creep strengths of Ni-based superalloys. Proceedings of the

International Symposium on Superalloys, (2008) 433-442.
[5] R.V. Miner, T.P. Gabb, J. Gayda, Orientation and temperature dependence of some mechanical properties of the single-crystal nickel-base superalloy René N4 III - Tension-compression anisotropy. Metallurgical Transactions A, 17 (1986) 507-512.
[6] S.S. Ezz, D.P. Pope, V. Paidar, The tension/compression flow stress asymmetry in Ni3(Al,Nb) Single crystals. Acta Metallurgica, 30 (1982) 921-926.
[7] D. Leidermark, J.J. Moverare, S. Johansson, K. Simonsson, S. Sjöström, Tension/compression asymmetry of a single-crystal superalloy in virgin and degraded condition. Acta Materialia, 58 (2010) 4986-4997.
[8] M. Segersäll, J.J. Moverare, K. Simonsson, S. Johansson, Deformation and damage mechanisms during thermomechanical fatigue of a single-crystal superalloy in the $\langle 001\rangle$ and $\langle 011\rangle$ directions. Proceedings of the International Symposium on Superalloys, (2012) 215-223.
[9] J.J. Moverare, S. Johansson, R.C. Reed, Deformation and damage mechanisms during thermal–mechanical fatigue of a single-crystal superalloy. Acta Materialia, 57 (2009) 2266-2276.
[10] J.X. Zhang, H. Harada, Y. Ro, Y. Koizumi, T. Kobayashi, Thermomechanical fatigue mechanism in a modern single crystal nickel base superalloy TMS-82. Acta Materialia, 56 (2008) 2975-2987.
[11] M. Dupeux, J. Henriet, M. Ignat, Tensile stress relaxation behaviour of Ni-based superalloy single crystals between 973 and 1273 K. Acta Metallurgica, 35 (1987) 2203-2212.
[12] H. Mughrabi, Microstructural aspects of high temperature deformation of monocrystalline nickel base superalloys: Some open problems. Materials Science and Technology, 25 (2009) 191-204.
[13] T.M. Pollock, A.S. Argon, Directional coarsening in nickel-base single crystals with high volume fractions of coherent precipitates, Acta Metallurgica et Materialia. 42 (1994) 1859-1874.
[14] U. Tetzlaff, H. Mughrabi, Enhancement of the High-Temperature Tensile Creep Strength of Monocrystalline Nickel-Base Superalloys by Pre-rafting in Compression. Proceedings of the International Symposium on Superalloys, (2000) 273-282.
[15] H. Mughrabi, U. Tetzlaff, Microstructure and high-temperature strength of monocrystalline nickel-base superalloys. Advanced Engineering Materials, 2 (2000) 319-326.
[16] M. Ott, H. Mughrabi, Dependence of the high-temperature low-cycle fatigue behaviour of the monocrystalline nickel-base superalloys CMSX-4 and CMSX-6 on the γ/γ'-morphology. Materials Science and Engineering: A, 272 (1999) 24-30.
[17] R.V. Miner, R.C. Voigt, J. Gayda, T.P. Gabb, Orientation and temperature dependence of some mechanical properties of the single-crystal superalloy René N4 Part I: Tensile behavior. Metallurgical Transactions A, 17 (1986) 491-496.
[18] T.S. Rong, Serrated yielding in the B2-ordered Nb–15Al–20V alloy. Intermetallics, 11 (2003) 151-155.
[19] X. Wu, J.H. Zhang, J.L. Liu, T. Jin, Y.B. Xu, Z.Q. Hu, Plastic deformation inhomogeneity in a single crystal nickel-base superalloy. Materials Science and Engineering: A, 325 (2002) 478-483.
[20] E.F. Westbrooke, L.E. Forero, F. Ebrahimi, Slip analysis in a Ni-base superalloy. Acta

Materialia, 53 (2005) 2137-2147.
[21] X. -H. Li, J. Moverare, The use of acoustic emission technology in coating ductility testing at various temperatures. Proceedings of ASME Turbo Expo (2004).